# Effects of Imperfections and Residual Inter-Qubit Interaction on Quantum Computing

*D.L. Shepelyansky, B. Georgeot, CNRS-Toulouse, France*
dima(…)irsamc.ups-tlse.fr / www.quantware.ups-tlse.fr

## Objective

- Effects of realistic imperfections on quantum computer operability and accuracy
- Quantum chaos and ergodicity induced by inter-qubit couplings
- New efficient algorithms for simulation of quantum and classical physical systems
- Development and test of error-correcting codes for quantum chaos and noisy gates

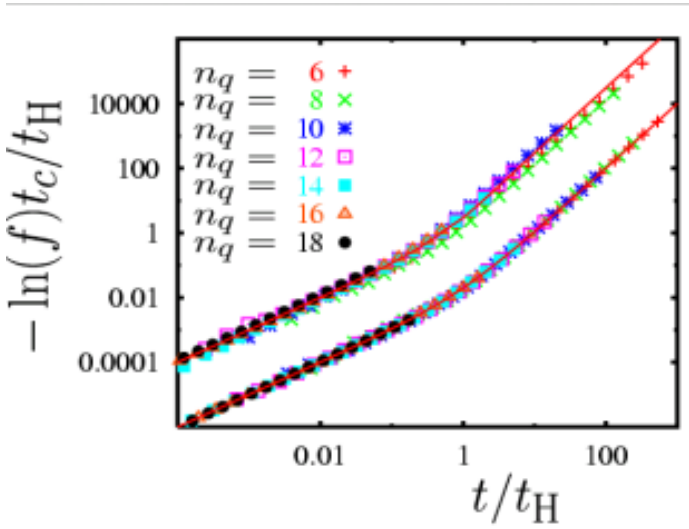


## Objective Approach

- Analytical methods developed for many-body systems (nuclei, atoms, quantum dots)
- Random matrix theory and quantum chaos
- Large-scale numerical simulations of many qubits on modern supercomputers
- Stability of algorithms to quantum errors

## Status

- Project period: May 2001– July 2004 (**poster**)
- Universal law for fidelity decay induced by static imperfections (random matrix theory)
- Quantum phase transition for the Grover algorithm due to inter-qubit interactions
- Quantum algorithm for kicked Harper model
- Gyroscopic quantum error correction method

# Effects of Imperfections and Residual Inter-Qubit Interaction on Quantum Computing

*D.L.Shepelyansky, B. Georgeot, CNRS-Toulouse, France*

- Progress on last year's objectives

- Random matrix theory is applied to quantum computations in presence of static imperfections; this gives the universal law for fidelity decay in quantum algorithms for complex dynamics; theory developed determines time scales for reliable quantum computations (related to the Heisenberg and Thouless time scales); numerical checks with up to 18 qubits for 10 orders of scaled fidelity variation
- Numerical and analytical study of stability of the Grover algorithm in presence of inter-qubit couplings; quantum phase transition border is determined for reliable algorithm operability
- Measurements effects for dynamical localization quantum algorithm
- Quantum algorithms for simulation of electrons in a magnetic field (kicked Harper model), static imperfection effects on transport, numerical tests with up to 15 qubits
- Gyroscopic method for quantum error correction of static imperfections is proposed and tested with up to 16 qubits
- 20 publications during the grant period

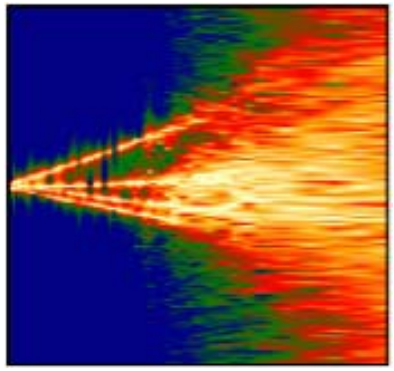

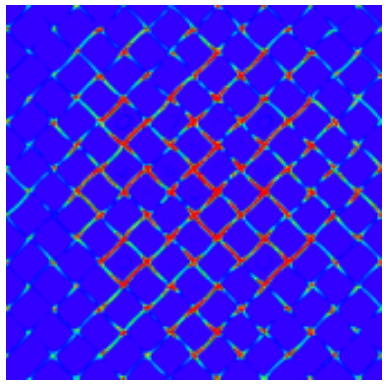

- Long term objectives

- New efficient algorithms modeling complex systems, accuracy and error-correcting codes in a realistic quantum computer

# Quantware group at Toulouse

Quantware MIPS Center, Laboratoire de Physique Théorique
UMR 5152 du CNRS, Université Paul Sabatier
Toulouse, France www.quantware.ups-tlse.fr

R.Fleckinger, K.Frahm (professors Univ. P.Sabatier)

B. Georgeot (researcher CNRS)

D.L. Shepelyansky (researcher CNRS, PI)

Jae-Weon Lee (postdoc, EC IST-FET project EDIQIP)

M.Terraneo (former postdoc, EU RTN project QTRANS)

A.Pomeransky (PhD student, US ARO/NSA/ARDA grant)

B.Lévi (PhD student, supported by French government)

A.Chepelianskii (undergraduate)

Collaboration: O.V.Zhirov (Budker Inst. of Nuclear Physics, Novosibirsk)

SUPPORT: ARO/NSA/ARDA program and EU IST-FET EDIQIP

# Quantum Hardware Melting Induced by Quantum Chaos

The quantum computer hardware is modeled as a (one)two-dimensional lattice of qubits (spin halves) with static fluctuations/imperfections in the individual qubit energies and residual short-range inter-qubit couplings. The model is described by the many-body Hamiltonian (B.Georgeot, D.S. PRE (2000)):

$$H_S = \sum_i (\Delta_0 + \delta_i)\sigma_i^z + \sum_{i<j} J_{ij}\sigma_i^x \sigma_j^x,$$

where the $\sigma_i$ are the Pauli matrices for the qubit $i$, and $\Delta_0$ is the average level spacing for one qubit. The second sum runs over nearest-neighbor qubit pairs, and $\delta_i$, $J_{ij}$ are randomly and uniformly distributed in the intervals $[-\delta/2, \delta/2]$ and $[-J, J]$, respectively. Quantum chaos border for quantum hardware:

$$J > J_c \approx \Delta_c \approx 3\delta/n_q \gg \Delta_n \sim \delta 2^{-n_q}$$

Emergency rate of quantum chaos: $\Gamma \sim J^2/\Delta_c$.

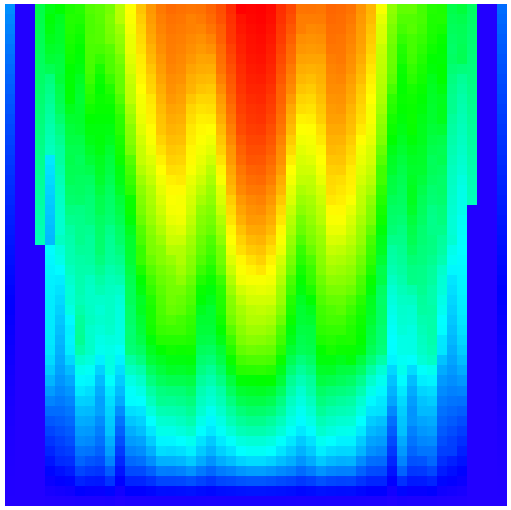

Quantum computer melting induced by inter-qubit couplings. Color represents the level of quantum eigenstate entropy $S_q$ (red for maximum $S_q \approx 11$, blue for minimum $S_q = 0$). Horizontal axis is the energy of the computer eigenstates counted from the ground state to the maximal energy ($\approx 2n_q\Delta_0$). Vertical axis gives the value of $J/\Delta_0$ (from $0$ to $0.5$). Here $n_q = 12$, $J_c/\Delta_0 = 0.273$, and one random realization of couplings is chosen.

What are effects of quantum many-body chaos
on the accuracy of quantum computations?
Static imperfections vs. random errors
in quantum gates of a quantum algorithm.

# Fidelity decay due to errors

Accuracy measure of quantum computation is fidelity: $f(t) = |<\psi(t)|\psi_\varepsilon(t)>|^2$ .

Quantum algorithm: $|\psi(t)> = U^t\,|\psi(0)>$ , $U = \underbrace{U_{N_g}\cdot\ldots\cdot U_1}_{\text{elementary gates}}$ .

Errors: $U_j \;\longrightarrow\; U_j\, e^{i\delta H}$ , $\delta H \sim \varepsilon$ .

**(i)** Decoherence due to residual couplings of quantum computer to external bath:

$\delta H$ random and different at each $j$ and $t$,

e.g.: random phase fluctuations: $\delta\phi \in [-\varepsilon, \varepsilon]$ in phase-shift gates.

**(ii)** Static imperfections in the quantum computer itself:

$\delta H$ (random but) constant at each $j$ and $t$,

e.g.: $\delta H = \sum_{j=0}^{n_q-1} \delta_j\, \sigma_j^{(z)} + 2\sum_{j=0}^{n_q-2} J_j\, \sigma_j^{(x)}\, \sigma_{j+1}^{(x)}$ , $J_j, \delta_j \in [-\varepsilon, \varepsilon]$ .

**(iii)** Non-unitary errors in quantum computation:

$e^{i\delta H}$ is non-unitary ($\delta H \neq \delta H^\dagger$, density matrix and quantum trajectories approach)

# Example: model of quantum tent map

$$H(t) = \frac{T\,p^2}{2} + V(\theta) \sum_{n=-\infty}^{\infty} \delta(t-n)$$

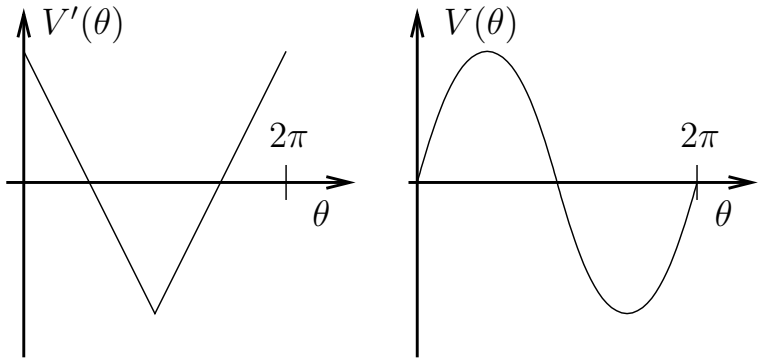


Classical map :

$$p_{n+1} = p_n - V'(\theta_n)$$
$$\theta_{n+1} = \theta_n + T\,p_{n+1}$$

Quantum map : $p = -i\partial/\partial\theta$

$$|\psi(t+1)> = U\,|\psi(t)>$$
$$U = e^{-iTp^2/2}\,e^{-iV(\theta)}$$

$$V(\theta) = \begin{cases} -\frac{k}{2}\theta(\theta-\pi) \\ \frac{k}{2}(\theta-\pi)(\theta-2\pi) \end{cases}, \quad V'(\theta) = \begin{cases} k(\frac{\pi}{2}-\theta) & \text{if} \quad 0 \le \theta \le \pi \\ k(-\frac{3\pi}{2}+\theta) & \text{if} \quad \pi \le \theta \le 2\pi \end{cases}$$

# Quantum algorithm for tent (and saw-tooth) map

Quantum register identification: $|p> \equiv |\alpha_0>_0 \, |\alpha_1>_1 \, \ldots \, |\alpha_{n_q-1}>_{n_q-1}$ .

$$p = \sum_{j=0}^{n_q-1} \alpha_j \, 2^j \;\in\; \{0, \ldots, N-1\}$$

$N = 2^{n_q}$ = dimension of Hilbert space; $n_q$ = number of qubits; $\alpha_j \;\in\; \{0, 1\}$.

Quantum Fourier transform: $p \leftrightarrow \theta$ and $e^{-iTp^2/2} \, |p> = \prod_{j<k} \underbrace{e^{i(\cdots)\alpha_j\alpha_k}}_{B^{(2)}_{jk}(\cdots)} \prod_j \underbrace{e^{i(\cdots)\alpha_j}}_{B^{(1)}_j(\cdots)} \, |p>$ .

with simple and controlled phase-shift:

$$B^{(1)}_j(\phi) = \begin{pmatrix} 1 & 0 \\ 0 & e^{i\phi} \end{pmatrix} \quad , \quad B^{(2)}_{jk}(\phi) = \begin{pmatrix} 1 & 0 & 0 & 0 \\ 0 & 1 & 0 & 0 \\ 0 & 0 & 1 & 0 \\ 0 & 0 & 0 & e^{i\phi} \end{pmatrix} .$$

Double controlled phase-shift: $B^{(3)}_{jkl}(\phi) = B^{(2)}_{jl}\left(\frac{\phi}{2}\right) \, B^{(2)}_{jk}\left(\frac{\phi}{2}\right) \, C^{(N)}_{kl} \, B^{(2)}_{jk}\left(-\frac{\phi}{2}\right) \, C^{(N)}_{kl}$ .

Number of elementary gates: $n_g \approx 9 \, n_q^2/2$

## Husimi function

$t = 5$ 16 qubits $t = 15$

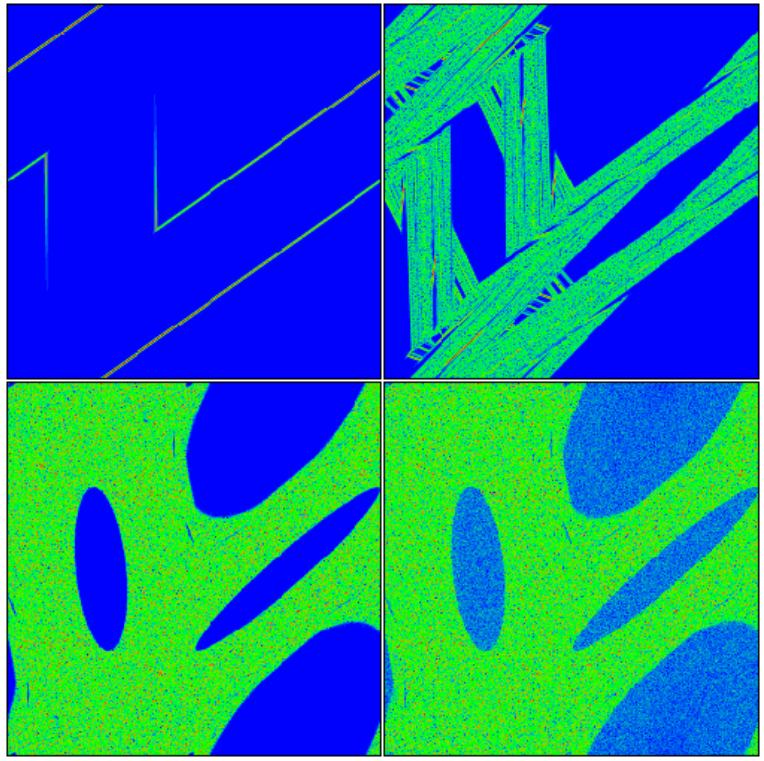

$t = 5625, \varepsilon = 0$ $\varepsilon = 7 \cdot 10^{-7}$

$\hbar_{\rm eff} = T = 2\pi/N, \;\; N = 2^{nq}$

## Poincaré section ($K = kT = 1.7$)

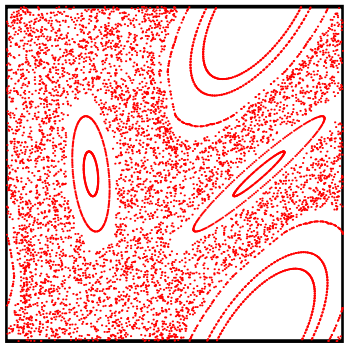

## Fidelity decay with errors

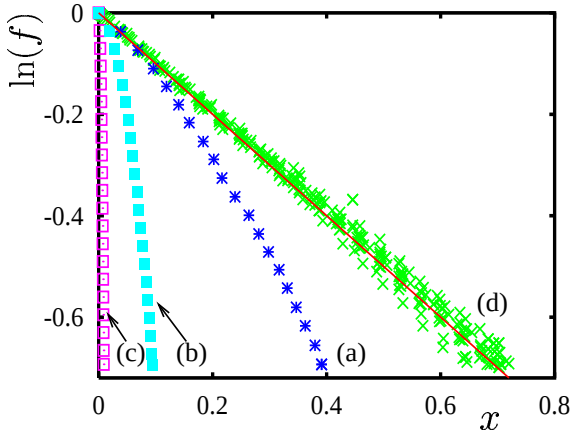


(static: $x = t/t_c$, (a), (b), (c),
random: $x = t/t_r$, (d))

# Random matrix theory for fidelity decay

Fidelity with average initial state: $f(t) = \left| \frac{1}{N} \mathtt{tr} \left( U^{-t} \left( U\, e^{i\delta H_{\rm eff}} \right)^t \right) \right|^2$

Regime $(1-f) \ll 1$ : $f(t) \approx 1 - \frac{t}{t_c} - \frac{2}{t_c} \sum_{\tau=1}^{t-1} (t-\tau)\, C(\tau)$

with: $\frac{1}{t_c} = \frac{1}{N} \mathtt{tr} \left( {\delta H_{\rm eff}}^2 \right)$ , $C(\tau) = \frac{t_c}{N} \mathtt{tr} \left( \underbrace{U^{-\tau}\, \delta H_{\rm eff}\, U^{\tau}}_{\delta H_{\rm eff}(\tau)}\, \delta H_{\rm eff} \right)$

$U \in$ COE (CUE) $\Rightarrow$ Scaling law:

$$-\langle \ln f(t) \rangle_U \approx \frac{N}{t_c} \chi \left( \frac{t}{N} \right) , \quad \chi(s) = s + \frac{2}{\beta}\, s^2 - 2 \int_0^s d\tilde{\tau}\, (s-\tilde{\tau})\, b_2(\tilde{\tau}) \, .$$

with the "two-level form factor": $b_2(\tilde{\tau})$.

# Scaling analysis for chaotic dynamics

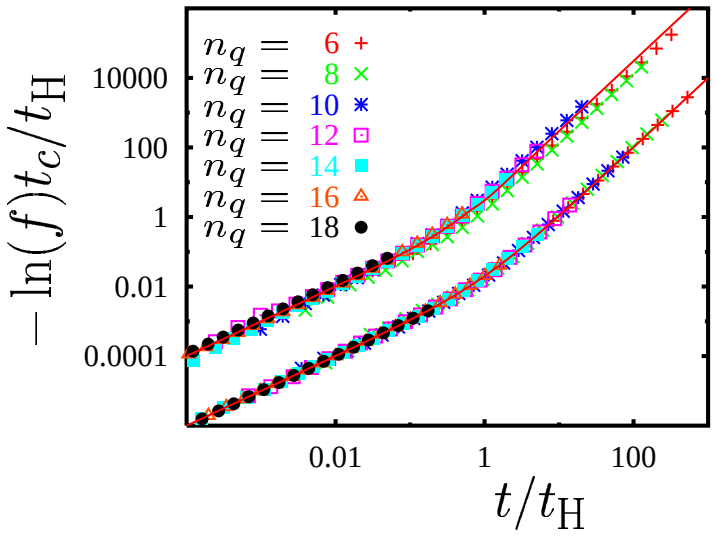


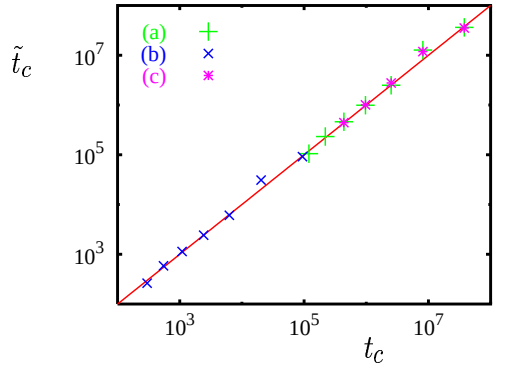


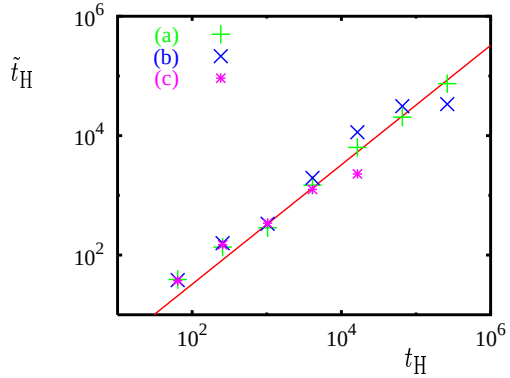


**Upper curve:** with theoretical values:

$t_{\rm H} = 2^{n_q}$ and $t_c = 1/(\varepsilon^2\, n_q\, n_g^2)$

**Lower curve:** with fit values $\tilde{t}_c$ and $\tilde{t}_{\rm H}$ from: $-\ln(f(t)) = \dfrac{t}{\tilde{t}_c} + \dfrac{t^2}{\tilde{t}_c \tilde{t}_{\rm H}} \quad (\tilde{t}_{\rm H} \approx t_{\rm H}/3)$

# Integrable dynamics

$t = 22783$ , Fit: $-\ln(f(t)) = \frac{t}{\tilde{t}_c} + \frac{t^2}{\tilde{t}_c \tilde{t}_{\rm H}}$ .

$n_q = 14$

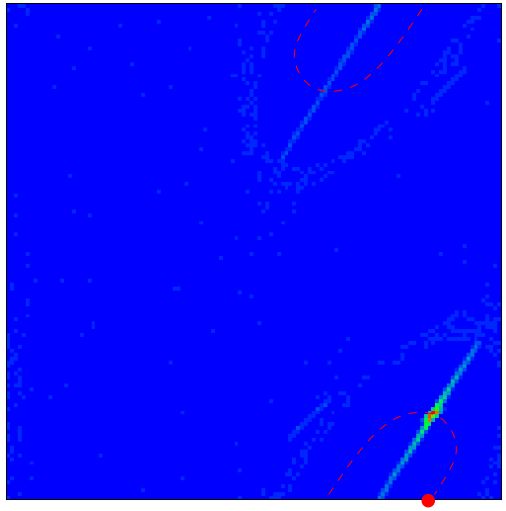

$\varepsilon = 0$

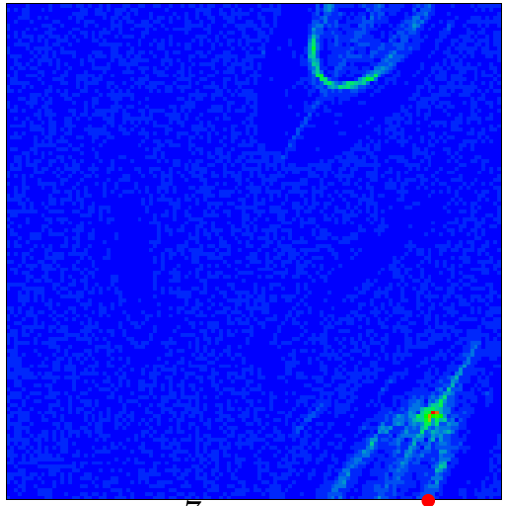

$\varepsilon = 5 \cdot 10^{-7}, \quad f = 0.5$

Position of initial gaussian wave packet

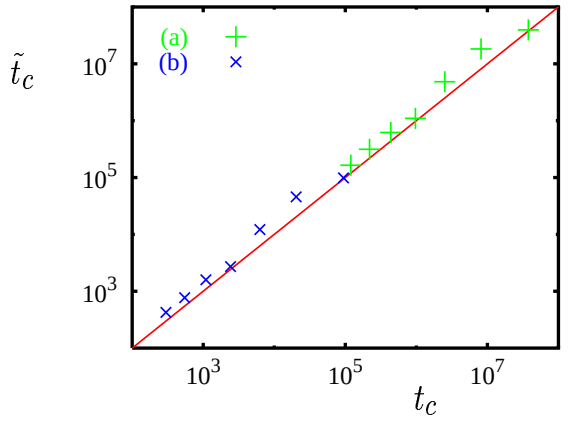


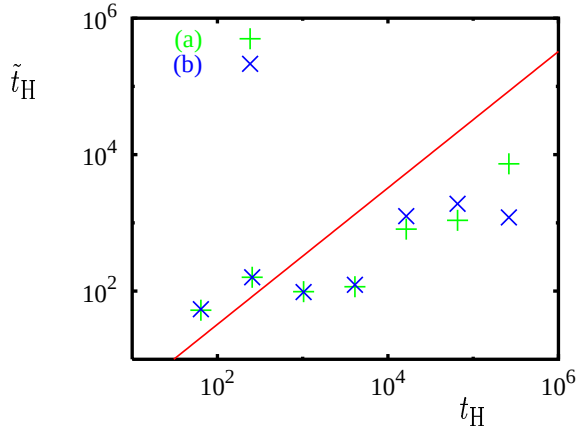

# Time scale of reliable quantum computations

Time scale $t_f$ with $f(t_f) = 0.9$ :

Theory from RMT-approach:

If $\varepsilon \gg (2^{n_q}\, n_g^2 n_q)^{-1/2}$:

$$t_f \approx 0.1\, t_c \approx 1/(10\varepsilon^2\, n_q\, n_g^2)$$

$$N_g = t_f\, n_g \approx 1/(10\varepsilon^2\, n_q\, n_g)$$

If $\varepsilon \ll (2^{n_q}\, n_g^2 n_q)^{-1/2}$:

$$t_f \approx 0.2\, \sqrt{t_c t_{\rm H}} \approx 2^{n_q/2}/(5\varepsilon\, n_g\, \sqrt{n_q})$$

Random errors: $N_g \approx 5/\varepsilon^2$

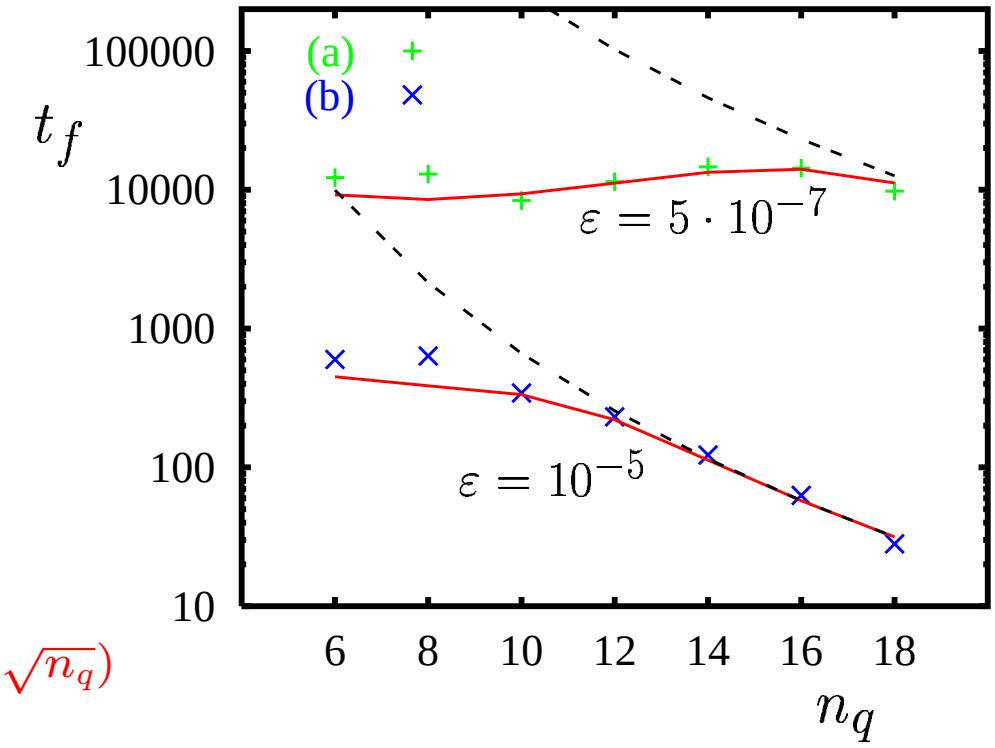

# Harper and kicked Harper models

Harper model: $H_0(p,q) = \cos(p) + \cos(q)$
fractal spectrum "Hofstadter butterfly" but integrable system
Kicked Harper model:
$H(p,q,t) = L\cos(p) + K\cos(q)\sum_n \delta(t-n)$
$\Rightarrow$ Transition to chaos as $K, L$ increase
integration over one period:
$\bar{n} = n + K\sin\theta\ ,\ \bar{\theta} = \theta - L\sin\bar{n}$
quantization:
$\bar{\psi} = \hat{U}\psi = e^{-iL\cos(\hbar\hat{n})/\hbar} e^{-iK\cos(\hat{\theta})/\hbar}\psi$
where $\hat{n} = -iq\partial/\partial\theta$ and $\psi(\theta + 2q\pi) = \psi(\theta)$.
$\Rightarrow$ Motion of electrons in EM fields
$\Rightarrow$ Stochastic heating of plasma

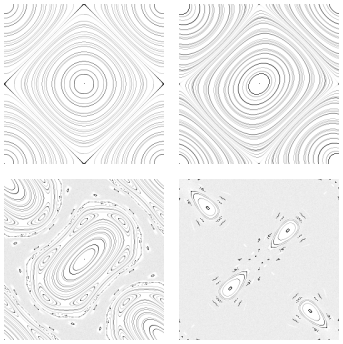

classical phase space

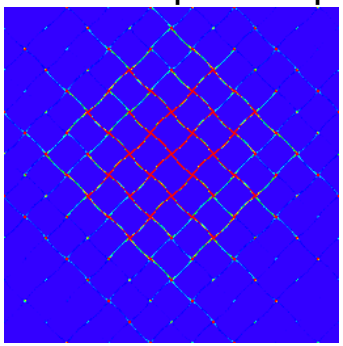

stochastic web

# localization properties

dynamical localization $\longrightarrow$ similar to Anderson localization of electrons in solids

transition to a partially delocalized regime, with coexistence of localized and delocalized states

Figure: Inverse Participation Ratio

$\xi = 1/\Sigma_n |\psi(n)|^4$

$\xi \approx l$ (localized state) $\longrightarrow$ $\xi \approx N$ (delocalized)

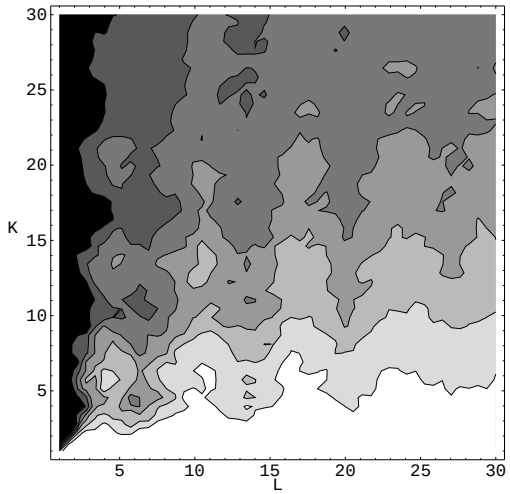


Exact algorithm (Georgeot and Shepelyansky, Physical Review Letters **86**, 2162 (2001)): needs $O(\log N_H^3)$ quantum gates for evolution of the wave function + workspace registers

$\Rightarrow$ More economical algorithms? Total complexity (including measurements)? Effects of static imperfections?

# Time-slice algorithm

$M(\alpha, U) = HC_U H e^{i\frac{\alpha}{2}\sigma_z} HC_{U^{-2}} H e^{i\frac{\alpha}{2}\sigma_z} HC_U H$

take $U = e^{ip\theta} \Rightarrow M(\alpha, U) \approx e^{i\alpha\cos(p\,\hat{\theta})}$

$e^{-ik\cos(p\,\hat{\theta})} \approx M(\alpha, U)^{n_s}$ with $\alpha = \frac{-k}{n_s}$ and error $O(\alpha^2)$

with $\widetilde{M}(\alpha, U) = M\left(\frac{\alpha}{2}, U\right) M\left(\frac{\alpha}{2}, U^{-1}\right)$,

then $e^{-ik\cos(p\,\hat{\theta})} \approx \widetilde{M}(\alpha, U)^{n_s}$ with error $O(\alpha^3)$

For KHM on $N_H = 2^{n_r}$ dimensional space:

$e^{-iK\cos(\hat{\theta})/\hbar}$ and $e^{-iL\cos(\hbar\hat{n})/\hbar} \Rightarrow 4 + 2(n_r - a) + (n_s - 1)(7 + 2(n_r - a))$ gates

QFT $\Rightarrow n_r^2$ gates

Only one ancilla qubit! $O(\log N_H)^2$ quantum gates

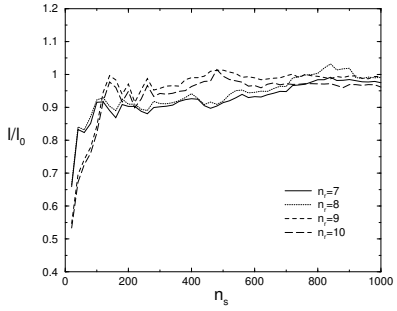


localization length

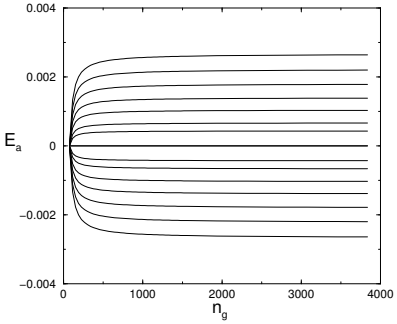


eigenphases

# Chebychev polynomials algorithm

$T_0(x) = 1, T_1(x) = x$, $T_n(x) = 2xT_{n-1}(x) - T_{n-2}(x)$

If $f(x)$ is a function on $[-1, 1]$, and $c_j = \frac{2}{M} \sum_{k=0}^{M-1} f\left[\cos\left(\frac{\pi\left(k+\frac{1}{2}\right)}{M}\right)\right] \cos\left(\frac{\pi j\left(k+\frac{1}{2}\right)}{M}\right)$

Then, for large $M$, $\sum_{j=0}^{M-1} c_j T_j(x) - \frac{1}{2}c_0$ is a very good approximation of $f(x)$ on $[-1, 1]$.

$P(x) \approx \cos(\pi(x+1)) \Rightarrow e^{-ik\cos(p\,\hat{\theta})} \approx e^{-ikP\left(\frac{\hat{\theta}}{\pi}-1\right)}$

Chebyshev polynomial approximation of degree $d \Rightarrow$ complexity is $O({n_r}^d)$. Numerics: $d = 6 \Rightarrow$ very good approximation of the wave function. $(N_H = 2^{n_r})$

Dropping the gates with the smallest phases shortens the computation keeping a reasonable accuracy.

No ancilla qubit! $O(\log N_H)^d$ quantum gates

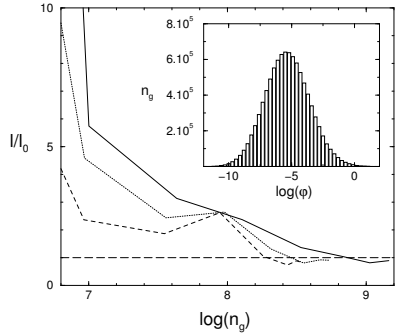


localization length

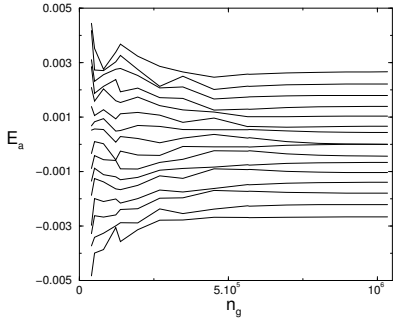


eigenphases

# Quantum stochastic web

$K, L$ very small $\Rightarrow$ small chaotic layer surrounding large integrable islands "stochastic web"

$\Rightarrow$ transport=diffusion through layer+tunneling

$\Rightarrow$ much faster than classical

Measuring diffusion constant:

$\Rightarrow$ Quantum computer: time evolution up to time $t^*$: $\sim t^*$ operations

$\Rightarrow$ Classical computer: time evolution up to a time $t^*$: $\sim t^*\sqrt{t^*}$ operations

$\Rightarrow$ Quantum gain (polynomial)

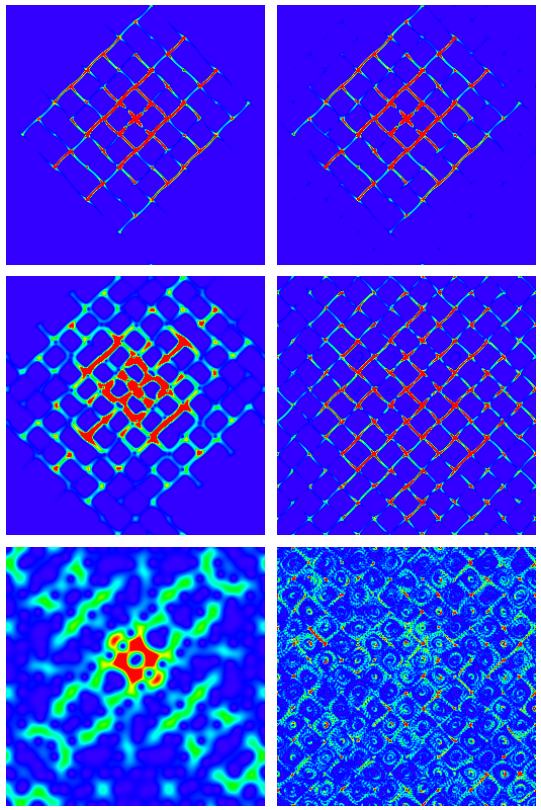

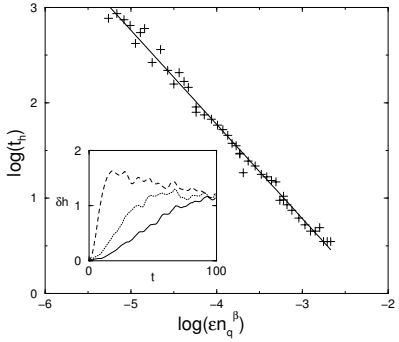


Effect of static errors: relative error is $1/2$ for $t_h \approx C_h/(\varepsilon n_q^{1.23})$

# Localized regime

Localization length $l$ measured directly by fitting an exponential function around maximal values of $\psi$, obtained by coarse grained measurement $\Rightarrow$ effective, no extra cost

Needs to evolve wave function until size $\approx l$

Short time $\Rightarrow$ diffusive spreading $\langle n(t)^2 \rangle \approx Dt$

wave packet needs to be evolved until a time $t^* \approx l^2/D$

Classically: to evolve a vector of dimension $\sim l$ until time $t^*$ $\Rightarrow \sim l^3$ classical operations.

Quantum computer: total number of gates $\sim l^2$.

$\Rightarrow$ polynomial improvement for the quantum algorithm.

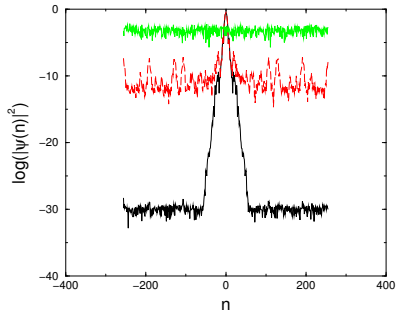


wave function

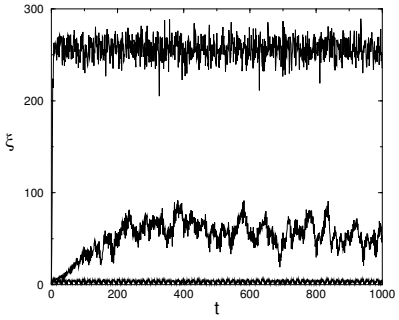


IPR vs time

# Localized regime: effect of static imperfections

$|\psi_a\rangle = \sum_{m=1}^{N} c_a^m |m\rangle$ eigenstates of exact evolution operator

Localized regime $\Rightarrow$ $|\psi_a\rangle$ localized $\Rightarrow$ the $c_a^m$ are significant only for $\sim l$ values of $m$, with $c_a^m \sim 1/\sqrt{l}$.

Matrix element of the imperfection Hamiltonian between $|\psi_a\rangle$'s:

$V_{typ} \sim \left| \langle \psi_b | \sum_{i=1}^{n_q} \delta_i \widehat{\sigma}_i^z \tau_g n_g | \psi_a \rangle \right| \sim \varepsilon n_g \sqrt{n_q}/\sqrt{l}$

$V_{typ} \sim \Delta_c$ (spacing between directly coupled states)

$\Rightarrow \varepsilon_c \approx C_1/(n_g\sqrt{n_q}\sqrt{l})$

Standard many body theory: $V_{typ} \gg \Delta_c \Rightarrow$ Fermi golden rule regime $\Rightarrow$ does not agree with numerics!

$\Rightarrow$ Gaussian regime, usually present for large $\varepsilon$

IPR is given by $\xi \sim \varepsilon n_g \sqrt{n_q} N$

$\varepsilon \ll \varepsilon_c \Rightarrow l$ can be measured for very long times

$\varepsilon \gg \varepsilon_c \Rightarrow l$ can be measured up to $t \sim 1/\sigma \sim 1/(\varepsilon n_g \sqrt{n_q})$

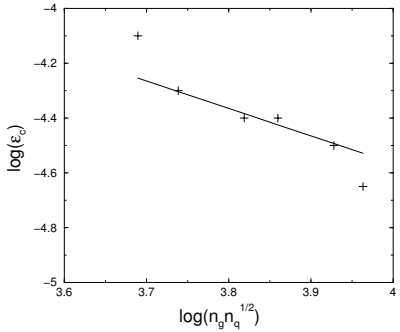


critical $\epsilon$

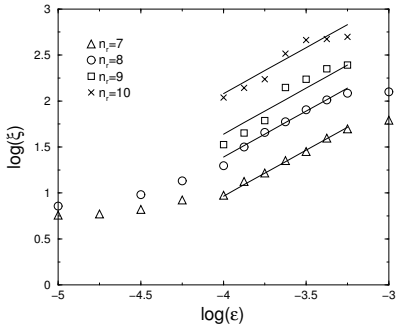


IPR vs $\epsilon$

# Partially delocalized regime

Coexistence of localized and delocalized wave functions; wave packet = localization peak + delocalization plateau

1) Measuring localization length:

Classical $\sim l^3$, quantum $\sim l^2$ as above

2) Measuring relative amplitude of plateau

$\Rightarrow$ evolve wave packet (WP) beyond size $\approx l$

$\Rightarrow$ classical $\sim l^3$, quantum $\sim l^2$

3) Diffusion constant of the plateau

a) away from $K = L$ line: anomalous diffusion (ballistic)

$\Rightarrow$ evolve WP up to time $t^*$: $\sim (t^*)^2$ classically, $\sim t^*$ quantum

b) on the $K = L$ line: normal diffusion

$\Rightarrow$ evolve WP up to time $t^*$: $\sim (t^*)^{3/2}$ classically, $\sim t^*$ quantum

$\Rightarrow$ polynomial improvement for the quantum algorithm.

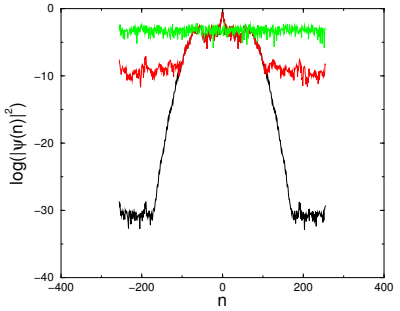


wave function

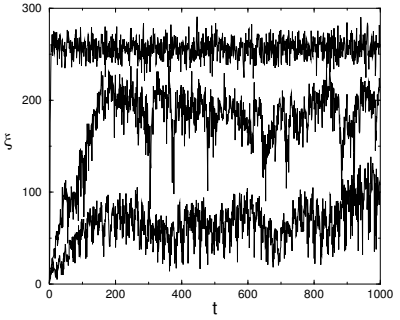


IPR vs time

# Partially delocalized regime: effect of static imperfections

$\beta N$ of the Floquet eigenstates $|\psi_a\rangle$ are delocalized. $|\psi_a\rangle = \sum_{m=1}^{N} c_a^m |m\rangle \Rightarrow$ the $c_a^m$ of have small nonzero values $\sim 1/\sqrt{N}$ for all $m$. $\Rightarrow V_{typ} \sim \varepsilon n_g \sqrt{n_q}/\sqrt{N}$

$V_{typ} \sim \Delta_c \Rightarrow \varepsilon_c \approx C_2/(n_g\sqrt{n_q}\sqrt{N})$

Exponentially small: $N = 2^{n_q}$!

Gaussian regime $\Rightarrow$ IPR grows like $\sigma/\Delta_n$, where $\sigma \sim \varepsilon n_g \sqrt{n_q}$ and $\Delta_n \sim 1/N$.

$\Rightarrow$ IPR $\sim \varepsilon n_g \sqrt{n_q} N$

$\Rightarrow$Transition point $\sim \varepsilon n_g \sqrt{n_q} N$ ($\neq$ Anderson transition)

$\varepsilon \gg \varepsilon_c \Rightarrow$ observables measurable up to time $t \sim 1/\sigma \sim 1/(\varepsilon n_g \sqrt{n_q})$

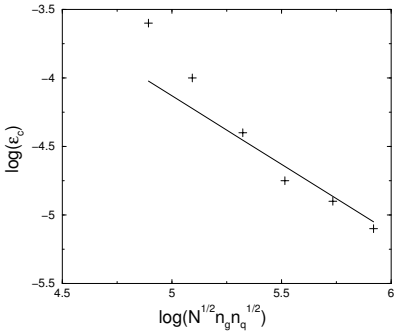


critical $\epsilon$

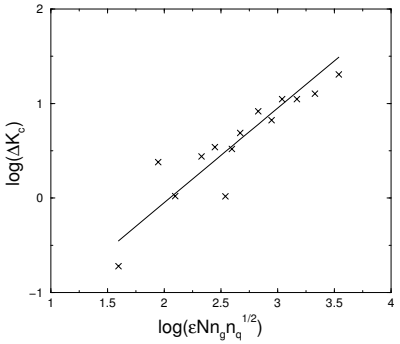


transition:scaling law

# spectrum: phase estimation + Grover

Start with $\sum_{t=0}^{N_H-1} |t\rangle|\psi_0\rangle$, with for example $|\psi_0\rangle = 2^{-n_r/2}\sum_n |n\rangle$
$\Rightarrow 2^{-n_r/2}\sum_{t=0}^{N_H-1} |t\rangle|U^t\psi_0\rangle$ in $O(N_H)$ operations,
QFT of the first register $\Rightarrow$ peaks centered at eigenvalues of $U$
measurement of the first register $\Rightarrow$ one eigenvalue of $U$ with good probability in $O(N_H)$ operations
amplitude amplification (Grover): all eigenvalues in a given interval in $O(N_H\sqrt{N_H})$ operations
Compare with $O(N_H^2)$ operations classically
Effects of static imperfections:
Time-slice method: error $\sim \varepsilon$
Chebychev method: error $\sim \varepsilon^{1.3}$

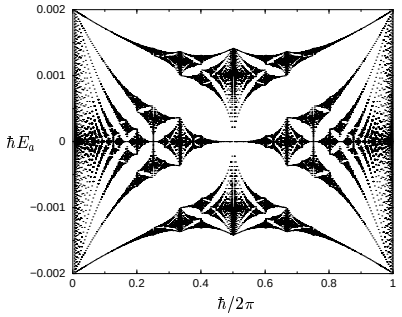


fractal spectrum

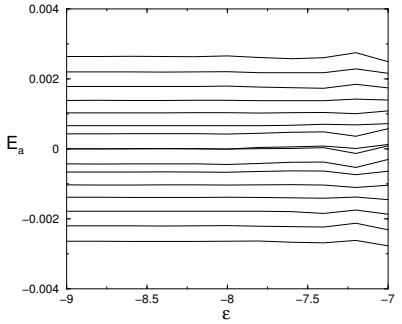


imperfection effects

# Phase diagram for the Grover algorithm with static imperfections

An unstructured database is presented by $N = 2^{n_q}$ states of quantum register with $n_q$ qubits: $\{|x\rangle\}$, $x = 0, \ldots, N-1$. The searched state $|\tau\rangle$ can be identified by *oracle* function $g(x)$, defined as $g(x) = 1$ if $x = \tau$ and $g(x) = 0$ otherwise. The Grover iteration operator $\hat{G}$ is a product of two operators: $\hat{G} = \hat{D}\hat{O}$. Here the oracle operator $\hat{O} = (-1)^{g(\hat{x})}$ is specific to the searched state $|\tau\rangle$, while the diffusion operator $\hat{D}$ is independent of $|\tau\rangle$: $D_{ii} = -1 + \frac{2}{N}$ and $D_{ij} = \frac{2}{N}$ $(i \neq j)$. For the initial state $|\psi_0\rangle = \sum_{x=0}^{N-1} |x\rangle/\sqrt{N}$, $t$ applications of the Grover operator $\hat{G}$ give:

$$|\psi(t)\rangle = \hat{G}^t|\psi_0\rangle = \sin\left((t+1)\omega_G\right)|\tau\rangle + \cos\left((t+1)\omega_G\right)|\eta\rangle$$

where the Grover frequency $\omega_G = 2\arcsin(\sqrt{1/N})$ and $|\eta\rangle = \sum_{x\neq\tau}^{(0\leq x<N)} |x\rangle/\sqrt{N-1}$. Hence, the ideal algorithm gives a rotation in the 2D plane $(|\tau\rangle, |\eta\rangle)$.

The implementation of the operator $D$ through the elementary gates requires an ancilla qubit. As a result the Hilbert space becomes a sum of two subspaces $\{|x\rangle\}$ and $\{|x+N\rangle\}$, which differ only by a value of $(n_q+1)$-th qubit. These subspaces are invariant with respect to operators $O$ and $D$: $O = 1 - 2|\tau\rangle\langle\tau| - 2|\tau+N\rangle\langle\tau+N|$, $D = 1 - 2|\psi_0\rangle\langle\psi_0| - 2|\psi_1\rangle\langle\psi_1|$, where $|\psi_1\rangle = \sum_{x=0}^{N-1}|x+N\rangle/\sqrt{N}$ and $|\psi_{0,1}\rangle$ correspond to up/down ancilla states. Then $D$ can be represented as $D = WRW$ (Grover (1997)), where the transformation $W = W_{nq}\ldots W_k\ldots W_1$ is composed from $n_q$ one-qubit Hadamard gates $W_k$, and $R$ is the $n_q$-controlled phase shift defined as $R_{ij} = 0$ if $i \neq j$, $R_{00} = 1$ and $R_{ii} = -1$ if $i \neq 0$ $(i,j = 0,\ldots,N-1)$. In turn, this operator can be represented as $R = W_{nq}\sigma^x_{nq-1}\ldots\sigma^x_1 \wedge_{nq} \sigma^x_{nq-1}\ldots\sigma^x_1 W_{nq}$, where $\wedge_{nq}$ is generalized $n_q$-qubit Toffolli gate, which inverts the $n_q$-th qubit if the first $n_q-1$ qubits are in the state $|1\rangle$. The construction of $\wedge_{nq}$ from 3-qubit Toffolli gates with the help of only one auxillary qubit is described by A.Barenco *et al.* (1995). As a result the Grover operator G is implemented through $n_g = 12n_{tot} - 42$ elementary gates including one-qubit rotations, control-NOT and Toffolli gates. Here $n_{tot} = n_q + 1$ is the total number of qubits.

# Oscillations of the Grover search probability

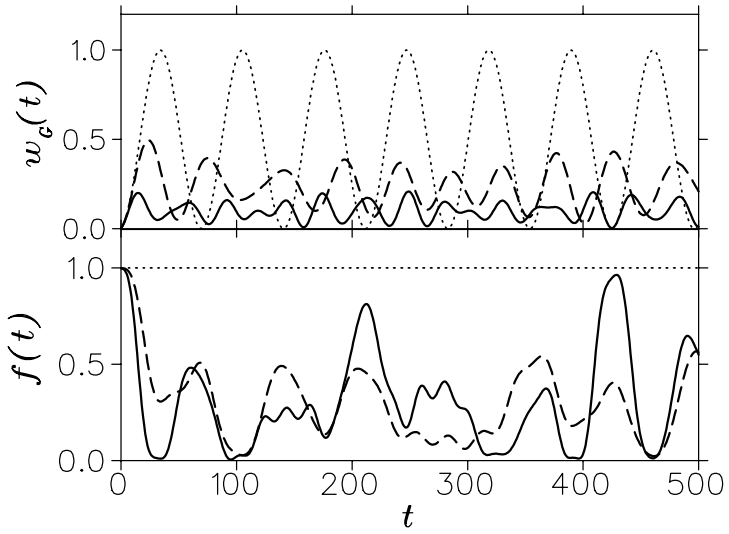


Probability of searched state $w_G(t)$ (top) and fidelity $f(t)$ (bottom) as a function of the iteration step $t$ in the Grover algorithm for $n_{tot} = 12$ qubits. Dotted curves show results for the ideal algorithm ($\varepsilon = 0$), dashed and solid curves correspond to imperfection strength $\varepsilon = 4 \cdot 10^{-4}$ and $10^{-3}$, respectively.

A typical example of imperfection effects on the accuracy of the Grover algorithm for a fixed disorder realization of $H_S$ on $3 \times 4$ qubit lattice.

# Husimi function in the Grover algorithm

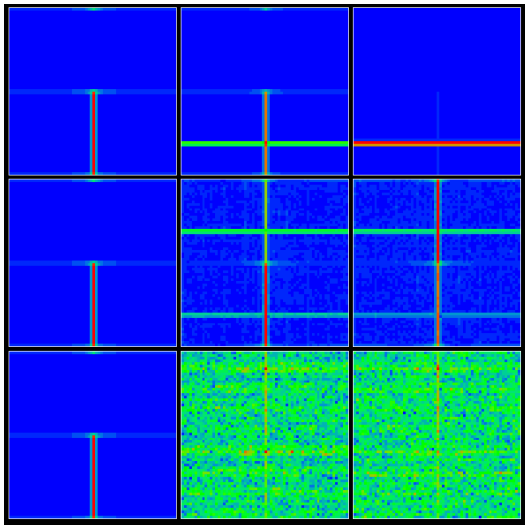

Evolution of the Husimi function in the Grover algorithm at times $t = 0$, 17, and $34$ (from left to right), and for $\varepsilon = 0$, 0.001, and 0.008 (from top to bottom). The qubit lattice and disorder realization are the same as in previous Fig. The vertical axis shows the computational basis $x = 0, \ldots, 2N - 1$, while the horizontal axis represents the conjugated momentum basis. Density is proportional to color changing from maximum (red) to zero (blue).

the probability is mainly distributed over four states corresponding to four straight lines in phase space: $|\tau_0\rangle = |\tau\rangle$ ; $|\tau_1\rangle = |\tau + N\rangle$ ; $|\eta_0\rangle = |\eta\rangle$ ; $|\eta_1\rangle = \sum_{x\neq\tau}^{(0\leq x<N)} |x + N\rangle/\sqrt{N-1}$

# Phase diagram for spectral density

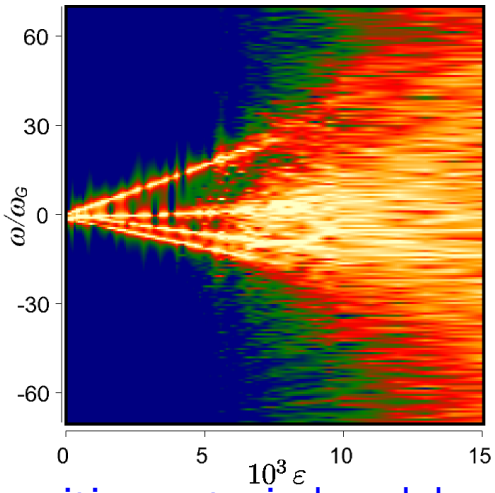


Phase diagram for the spectral density $S(\omega)$ as a function of imperfection strength $\varepsilon$, $n_{tot} = 12$, same disorder realization as in previous Fig. Color is proportional to density $S(\omega)$ (yellow for maximum and blue for zero).

The transition rate induced by imperfections after one Grover iteration is given by the Fermi golden rule: $\Gamma \sim \varepsilon^2 n_g^2 n_{tot}$, where $n_{tot}$ appears due to random contribution of qubit couplings $\varepsilon$ while $n_g^2$ factor takes into account coherent accumulation of perturbation on $n_g$ gates used in one iteration. In the Grover algorithm the four states are separated from all other states by energy gap $\Delta E \sim 1$ (sign change introduced by operators $O$ and $D$). Thus these four states become mixed with all others for $\varepsilon > \varepsilon_c \approx 1.7/(n_g\sqrt{n_{tot}})$, when $\Gamma > \Delta E$.

# Averaging over disorder

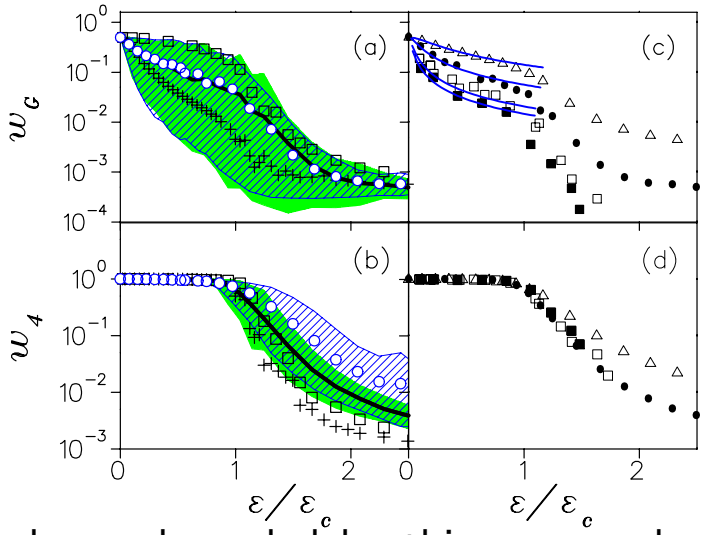


Dependence of probabilities $w_G$ (a,c) and $w_4$ (b,d) on rescaled imperfection strength $\varepsilon/\varepsilon_c$. For panels (a,b) $n_{tot} = 12$, squares and pluses show data for two typical disorder realizations, green/grey area shows the region of probability variation for various disorder realizations (see text), full thick curves give average dependence $\bar{w}_G$, $\bar{w}_4$.

Dashed area bounded by thin curves show the region of probability variation in the single-kick model, open circles give the average data in this model with rescaling factor $R = 0.56$. Panels (c,d) show $\bar{w}_G$, $\bar{w}_4$ for $n_{tot} = 9$ (triangles), 12 (full circles), 15 (open squares) and 16 (full squares). In panel (c) full curves are given by theory for same $n_{tot}$ values from top to bottom, $R = 0.56$.

# Theoretical estimates for the Grover algorithm (GA)

In the regime where the dynamics of Grover algorithm is dominated by four states subspace the single-kick model can be treated analytically. The matrix elements of the effective Hamiltonian in this space are

$$H_{eff} = \begin{pmatrix} A+a & 0 & -i\omega_G & 0 \\ 0 & A-a & 0 & -i\omega_G \\ i\omega_G & 0 & B & b \\ 0 & i\omega_G & b & B \end{pmatrix}, \quad (1)$$

where $A = -Rn_g \sum_{i=1}^{n_q} a_i \langle\tau|\sigma_i^{(z)}|\tau\rangle$, $B = Rn_g \sum_{i<j}^{n_q} b_{i,j} - b$, $a = -Rn_g a_{nq+1}$ and $b = Rn_g(b_{nq+1,nq+2-Lx} + b_{nq+1,Lx} + b_{nq,nq+1} + b_{nq+1-Lx,nq+1})$ and qubits are arranged on $L_x \times L_y$ lattice, and numerated as $i = x + L_x(y-1)$, with $x = 1, \ldots, L_x$, $y = 1, \ldots, L_y$. In the limit of large $n_q$ the terms $a, b$ are small compared to $A, B$ by a factor $1/\sqrt{n_q}$ and $H_{eff}$ is reduced to $2 \times 2$ matrix, which gives $w_G = 2\omega_G^2/[(A-B)^2 + 4\omega_G^2]$.

For large $n_q$ the difference $A-B$ has a Gaussian distribution with width $\sigma = Rn_g\sqrt{n_q/3}\sqrt{\alpha^2+2\beta^2} = \varepsilon Rn_g\sqrt{n_q}$. The convolution of $w_G$ with this distribution gives

$$\bar{w}_G = \sqrt{\pi/2}(1-erf(\sqrt{2}\omega_G/\sigma))\exp\left(2\omega_G^2/\sigma^2\right)\omega_G/\sigma \qquad (2)$$

This formula gives a good description of numerical data in Fig. c that confirms the validity of single-kick model. For $\sigma \gg \omega_G$ and a typical disorder realization with $(A-B) \sim \sigma$ the actual frequency of Grover oscillations is strongly renormalized: $\omega \approx (A-B) \sim \sigma \gg \omega_G$, and in agreement with previous Fig. $\omega \sim \varepsilon/\varepsilon_c$. In this typical case $w_G \sim \omega_G^2/\sigma^2 \ll 1$ (almost total probability is in the states $|\eta_0\rangle$,$|\eta_1\rangle$). Hence, the total number of quantum operations $N_{op}$, required for detection of searched state $|\tau\rangle$, can be estimated as $N_{op} \sim N_M/\omega \sim \sigma/\omega_G^2 \sim \varepsilon N/\varepsilon_c$, where $N_M \sim 1/w_G \sim \sigma^2/\omega_G^2$ is a number of measurements required for detection of searched state. Thus, in presence of strong static imperfections the parametric efficiency gain of the Grover algorithm compared to classical one is of the order $\varepsilon_c/\varepsilon$. For $\varepsilon \sim \omega_G$ the efficiency is comparable with that of the ideal Grover algorithm while for $\varepsilon \sim \varepsilon_c$ there is no gain compared to the classical case.

# Gyroscopic quantum error correction (GYQEC)

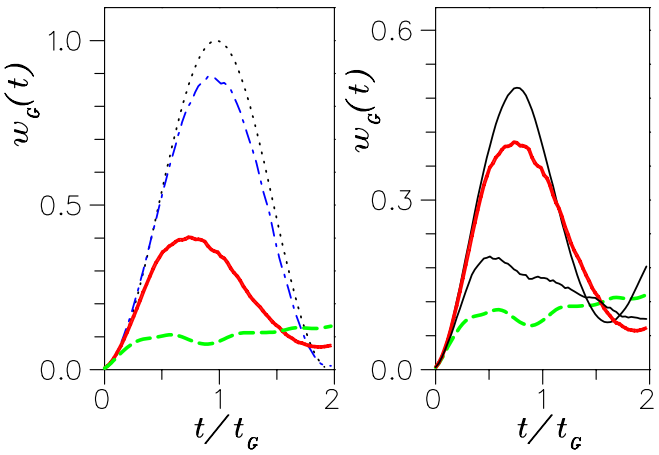


Probability $w_G(t)$ of a searched state in GA at $n_{tot} = 12, \varepsilon = 0.002, t_G = 34.5$. Left: curves show data for ideal GA, GA with gate to gate randomly fluctuating coupling coefficients $a_i, b_{ij}$, GYQEC with $l_g = 10$, GA with static imperfections (from top to bottom at $t/t_g = 1$). Right: curves show data for GYQEC at $l_g = 1, 10, 20$ and GA with static imperfections (top to bottom).

GYQEC is based on a random change of numeration of qubits after $l_g$ quantum gates. Namely, after $l_g$ gates about $n_{tot}/2$ swap operations are performed between random pairs of qubits so that the initial numeration of qubits is replaced by completely random one. However, in the quantum computer code this change is taken into account and the algorithm continues to run with new qubit numeration.

# Gyroscopic quantum error correction: Husimi image

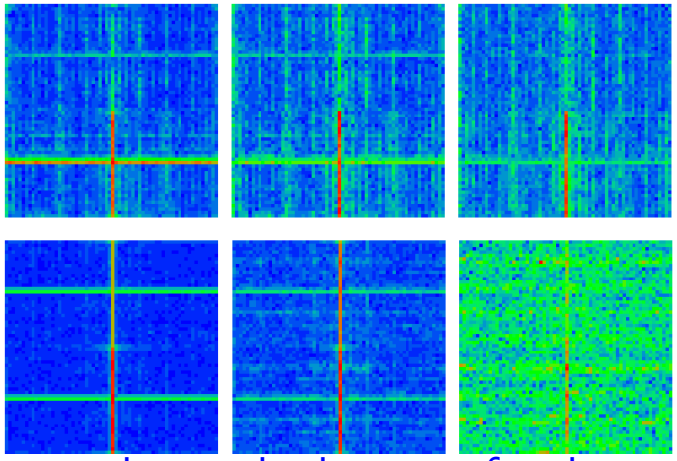

Husimi function in GA, shown at moment $t \sim t_G$ when $w_G(t)$ has maximum , for $\varepsilon = 0.002, 0.004, 0.008$ (left to right respectively); $n_{tot} = 12$. Top (bottom) row corresponds to the computation with (without) GYQEC at $l_g = 1$. Density is proportional to color changing from blue/zero to red/maximum.

In a sense the method uses a freedom of numeration of qubits in the program code and makes gyroscopic random rotations between all possibilities. These rotations suppress the effects of static imperfections. For Husimi function GYQEC gives a significant increase of the probability of searched state corresponding to lower horizontal line in a phase space square.

# Gyroscopic quantum error correction: probability decay

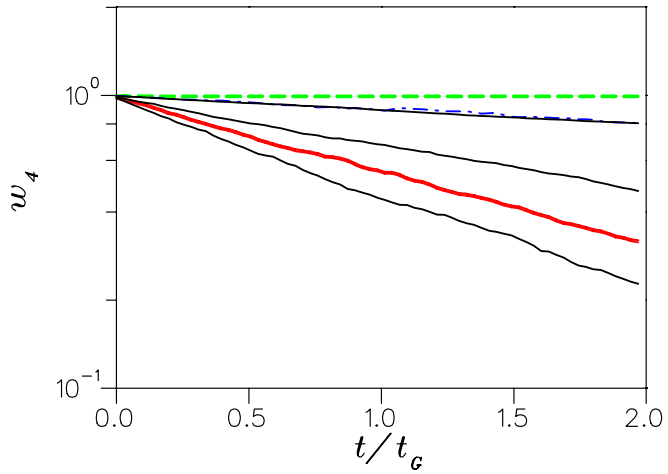


Probability $w_4(t)$ in the four states as a function of iteration time $t$ for $n_{tot} = 12, \varepsilon = 0.002, t_G = 34.5$. From top to bottom, curves show data without GYQEC, with time fluctuating couplings, with GYQEC at $l_g = 1$ (practically coincides with the previous curve) and at $l_g = 5, 10, 20$.

We note that the static imperfections preserve the total probability $w_4$ in 4-states until $\varepsilon < \varepsilon_c$ while time fluctuations of couplings $a_i, b_{ij}$ and GYQEC method give an exponential time decay of $w_4$ with a rate $\Gamma \propto \varepsilon^2$. In spite of this decay we obtain the accuracy gain.

# Gyroscopic quantum error correction: gain factor

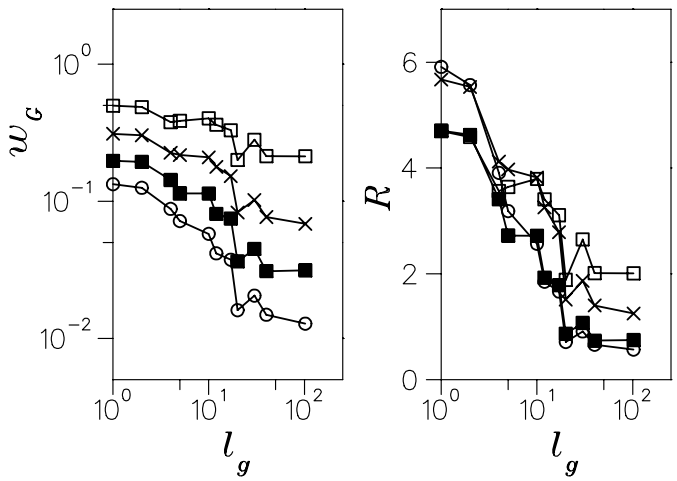


Left: probability $w_G$, averaged over 10 disorder realizations of static imperfections and taken at maximum, for $\varepsilon = 0.002, 0.003, 0.004, 0.005$, computation with GYQEC at different $l_g$ (top to bottom). Right: the gain factor $R$ given by the ratio of $w_G$ (from left) to its maximum value obtained in computations without GYQEC (same symbols). Here $n_{tot} = 12$.

The variation of the searched probability $w_G$ with $l_g$ is shown for various values of $\varepsilon$. GYQEC gives a maximal improvement of accuracy at minimal $l_g = 1$ when the effect of randomization of static imperfections becomes maximal. At $l_g = 1, n_{tot} = 12$ we reach the maximal accuracy gain factor $R \approx 6$ which it is not very sensitive to $\varepsilon$ in a certain range. We expect that this $R$ value will grow with the number of qubits $n_{tot}$.

# Pauli Random Error Correction (PAREC)

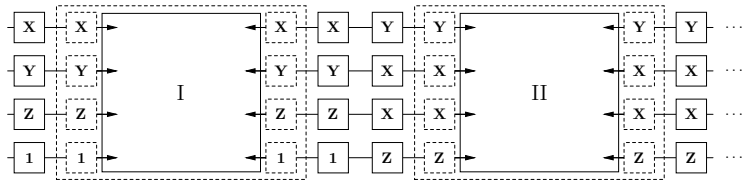


The basic idea of the PAREC-method: The two boxes (full lines) represent two sequences of universal quantum gates for $n_q = 4$ qubits. Two random sequences of Pauli operators $(\hat{X}_1, \hat{Y}_2, \hat{Z}_3, \mathbf{1}_4)$ and $(\hat{Y}_1, \hat{X}_2, \hat{X}_3, \hat{Z}_4)$ are also indicated. The unitary Pauli operators outside the dashed boxes (full lines) are applied to the qubits whereas the ones inside the dashed boxes (dashed lines) are taken into account by appropriate permutations of the elementary quantum gates. Due to the identities $\hat{X}^2 = \hat{Y}^2 = \hat{Z}^2 = \mathbf{1}$ the inserted random sequences of Pauli operators change the computational basis but leave the ideal quantum algorithm unchanged.

The PAREC method eliminates coherent errors produced by static imperfections and increases significantly the maximum time over which realistic quantum computations can be performed reliably. Furthermore, it does not require redundancy using all qubits for logical purposes.

# Pauli Random Error Correction (PAREC)

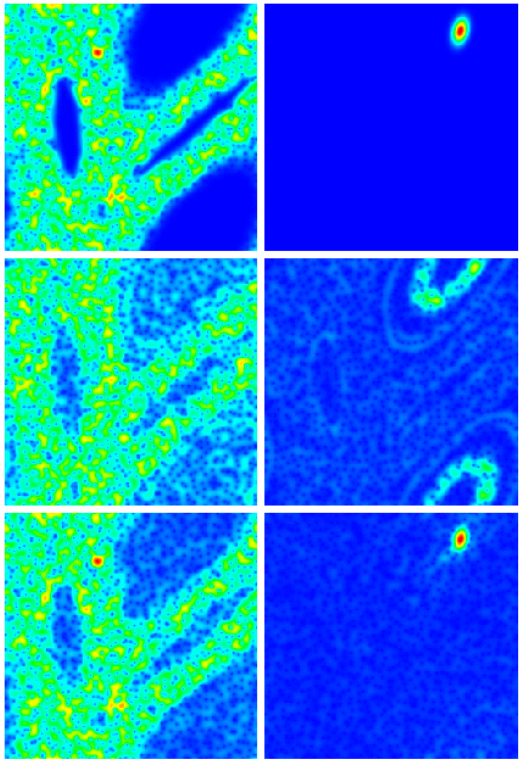

Quantum Poincaré sections with Husimi-functions in tent map at $t = 3000$ in scaled momentum and position variables $\tilde{y} = p \in [0, 2\pi]$ and $\tilde{x} = x \in [0, 2\pi]$: The parameters are $K = 1.7$ and $n_q = 10$. The initially prepared coherent states are centered around $(\pi/4, 0)$ (left panel) and $(5.35, 0)$ (right panel). First row: ideal dynamics; second row: static imperfections with $\epsilon = 5 \times 10^{-6}$; third row: PAREC-method applied after each sequence of $n_{\rm gef} = 20$ universal quantum gates of Ref. [17]. The probability density is coded in colors (red/maximum, blue/zero).

# Pauli Random Error Correction (PAREC)

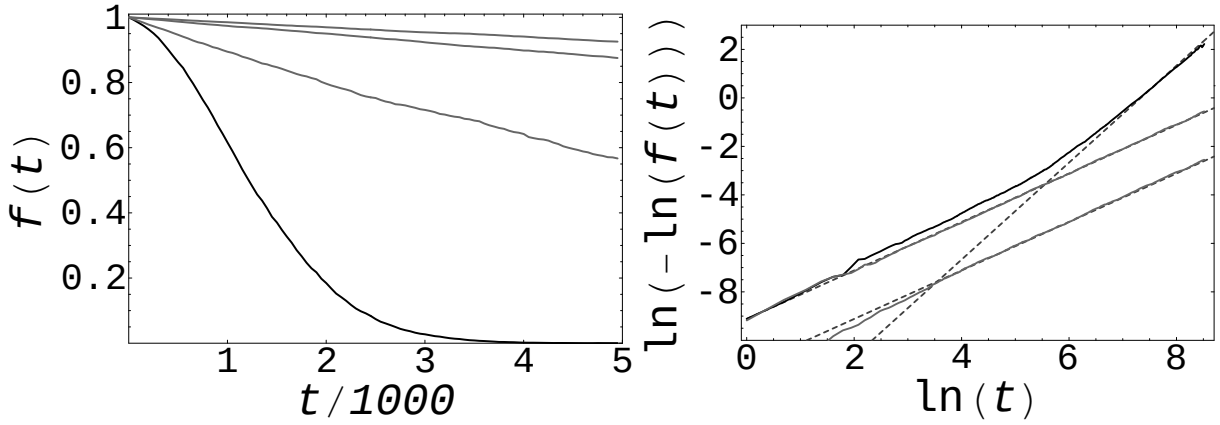


Dependence of the fidelity $f(t)$ on the number of iterations: Parameters as in the left panel of previous Fig.; left: static imperfections without error correction, PAREC after each map iteration, after each $n_{\rm gef} = 50$, and after each $n_{\rm gef} = 20$ quantum gates (from bottom up); right: static imperfections without error correction, with PAREC after each map iteration and after each sequence of $n_{\rm gef} = 20$ quantum gates (full curves), best fits for linear- and quadratic-in-time decays (dashed curves).

## A.N.Kolmogorov 25 April 1903 - 20 October 1987

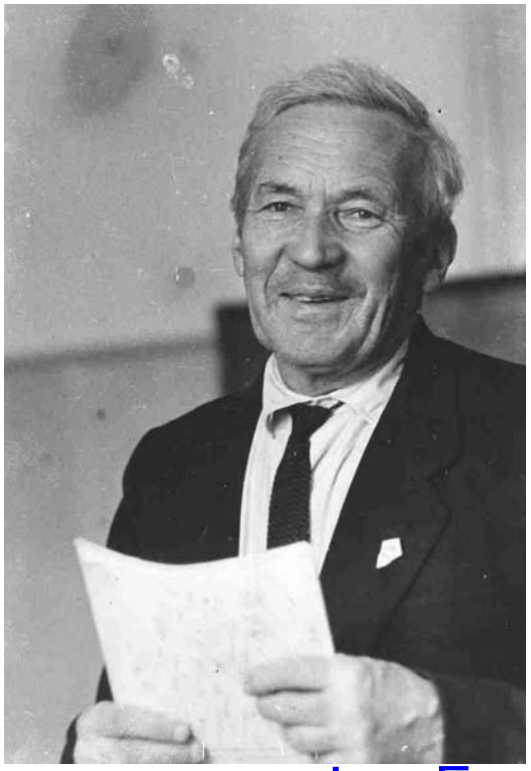

"Une vrai révolution s'est produite dans le domaine de la technologie des calcul dix ans auparavant. Il a été démontré qu'on peut se passer du déplacement méchanique des éléments de la machine de calcul en les remplaçant par des lampes électriques."
A.N.Kolmogorov "La profession du mathématicien", Université de Moscou, (1959)

New step: moving Entanglement !

# Grant publications (2001/05 to 2004/07)


1. G.Benenti, G.Casati and D.L.Shepelyansky, "Emergence of Fermi-Dirac thermalization in the quantum computer core", Eur. Phys. J. **D 17** (2001), 265 (quant-ph/0009084).
2. G.Benenti, G.Casati, S.Montangero and D.L.Shepelyansky, "Efficient quantum computing of complex dynamics", Phys. Rev. Lett. **87** (2001) 227901 [Fig.1 is on the cover page of Phys. Rev. Lett. of 26 Nov 2001] (quant-ph/0107036).
3. B.Georgeot and D.L.Shepelyansky, "Quantum computer inverting time arrow for macroscopic systems", Eur. Phys. J. **D 19** (2002), 263 (quant-ph/0105149).
4. B.Georgeot and D.L.Shepelyansky, Reply, Phys. Rev. Lett. **88** (2002), 219802 (quant-ph/0110142).
5. G.Benenti, G.Casati, S.Montangero and D.L.Shepelyansky, "Eigenstates of operating quantum computer: hypersensitivity to static imperfections", Eur. Phys. J. **D 20** (2002), 293 (quant-ph/0112132).
6. M.Terraneo, B.Georgeot and D.L.Shepelyansky, "Strange attractor simulated on a quantum computer", Eur. Phys. J. **D 22** (2003), 127 (quant-ph/0203062).
7. G.Benenti, G.Casati, S.Montangero and D.L.Shepelyansky, "Statistical properties of eigenvalues for an operating quantum computer with static imperfections", Eur. Phys. J. **D 22** (2003), 285 (quant-ph/0206130).
8. A.D.Chepelianskii and D.L.Shepelyansky, "Simulation of chaos-assisted tunneling in a semiclassical regime on existing quantum computers " Phys. Rev. **A 66** (2002), 054301 (quant-ph/0202113).
9. G.Benenti, G.Casati, S.Montangero and D.L.Shepelyansky, "Dynamical localization simulated on a few qubits quantum computer", Phys. Rev. **A 67** (2003), 052312 (quant-ph/0210052).
10. B.Lévi, B.Georgeot and D.L.Shepelyansky, "Quantum computing of quantum chaos in the kicked rotator model", Phys. Rev. **E 67** (2003), 046220 (quant-ph/0210154).

11. S.Bettelli and D.L.Shepelyansky, "Entanglement versus relaxation and decoherence in a quantum algorithm for quantum chaos", Phys. Rev. **A 67** (2003), 054303 (quant-ph/0301086).
12. M.Terraneo and D.L.Shepelyansky, "Imperfection effects for multiple applications of the quantum wavelet transform ", Phys. Rev. Lett. **90** (2003), 257902 (quant-ph/0303043).
13. A.A.Pomeransky, " Strong superadditivity of the entanglement of formation follows from its additivity ", Phys. Rev. **A 68** (2003), 032317 (quant-ph/0305056).
14. A.A.Pomeransky and D.L.Shepelyansky, "Quantum computation of the Anderson transition in presence of imperfections ", Phys. Rev. **A 69** (2004), 014302 (quant-ph/0306203)
15. J.W.Lee, A.D.Chepelianskii and D.L.Shepelyansky, "Treatment of sound on quantum computers ", submitted (quant-ph/0309018)
16. M.Terraneo and D.L.Shepelyansky, "Dynamical localization, measurements and quantum computing ", Phys. Rev. Lett. **92** (2004), 037902 (quant-ph/0309192)
17. K.M.Frahm, R.Fleckinger and D.L.Shepelyansky, "Quantum chaos and random matrix theory for fidelity decay in quantum computations with static imperfections ", Eur. Phys. J. **D 29** (2004), 139 [highlight paper of the issue] (quant-ph/0312120)
18. A.Stotland, A.A.Pomeransky, E.Bachmat and D.Cohen, "The information entropy of quantum mechanical states ", to appear in Europhys. Lett. (quant-ph/0401021).
19. A.A.Pomeransky, O.V.Zhirov and D.L.Shepelyansky, "Phase diagram for the Grover algorithm with static imperfections ", to appear in Eur. Phys. J. D (quant-ph/0403138).
20. B.Lévi and B.Georgeot, "Quantum computing of a complex system: the kicked Harper model", submitted.
21. A.A.Pomeransky, O.V.Zhirov and D.L.Shepelyansky, "Effects of decoherence and imperfections for quantum algorithms", contribution to ERATO Conference, Tokyo, 2004, submitted (quant-ph/0407264).
22. O.Kern, G.Alber and D.L.Shepelyansky, "Quantum error correction of coherent errors by randomization", submitted to Phys. Rev. Lett. (quant-ph/0407262).